

TABLE 3. Elastic Wave Velocities

Core Density, g/cm <sup>3</sup>	Direction of Wave Propagation	Direction of Wave Displacement	Notation	Velocity Relation	Velocity, km/sec					
					1.0 kb	2.0 kb	4.0 kb	6.0 kb	8.0 kb	10.0 kb
<i>Dunite A (x<sub>3</sub> axis//to symmetry axis)</i>										
3.260	[001]	[001]	V <sub>A1</sub>	$\rho V^2 = c_{33}$	8.568	8.622	8.688	8.726	8.750	8.762
		[100]	V <sub>A2</sub>	$\rho V^2 = c_{44}$	4.507	4.530	4.560	4.578	4.589	4.597
		[010]	V <sub>A3</sub>	$\rho V^2 = c_{44}$	4.506	4.531	4.565	4.587	4.595	4.598
		[100]	V <sub>A4</sub>	$\rho V^2 = c_{11}$	7.854	7.896	7.946	7.972	7.992	8.007
		[010]	V <sub>A5</sub>	$\rho V^2 = \frac{1}{2}(c_{11} - c_{12})$	4.352	4.381	4.414	4.430	4.440	4.447
3.248	[010]	[001]	V <sub>A6</sub>	$\rho V^2 = c_{44}$	4.572	4.599	4.635	4.660	4.671	4.677
		[010]	V <sub>A7</sub>	$\rho V^2 = c_{11}$	7.797	7.839	7.896	7.922	7.945	7.957
		[100]	V <sub>A8</sub>	$\rho V^2 = c_{44}$	4.597	4.621	4.643	4.657	4.667	4.676
		[110]	V <sub>A9</sub>	$\rho V^2 = \frac{1}{2}(c_{11} - c_{12})$	4.319	4.341	4.375	4.393	4.400	4.405
		[110]	V <sub>A10</sub>	$\rho V^2 = c_{11}$	7.769	7.813	7.857	7.884	7.900	7.912
3.269	[110]	[001]	V <sub>A11</sub>	$\rho V^2 = \frac{1}{2}(c_{11} - c_{12})$	4.344	4.360	4.379	4.392	4.402	4.415
		[110]	V <sub>A12</sub>	$\rho V^2 = c_{44}$	4.577	4.618	4.665	4.683	4.694	4.696
		[110]	V <sub>A13</sub>	$\rho V^2 = c_{11}$	7.852	7.905	7.965	8.001	8.026	8.046
		[110]	V <sub>A14</sub>	$\rho V^2 = c_{44}$	4.279	4.304	4.335	4.350	4.358	4.362
		[001]	V <sub>A15</sub>	$\rho V^2 = \frac{1}{2}(c_{11} - c_{12})$	4.617	4.647	4.677	4.687	4.689	4.691
3.286 3.256	[011] [101]	Quasi-long. Quasi-long.	V <sub>A16</sub> V <sub>A17</sub>	$\rho V^2 = c_{44}$ <i>a</i> <i>a</i>	8.339 8.346	8.383 8.393	8.444 8.464	8.481 8.508	8.501 8.530	8.504 8.536
<i>Dunite B</i>										
3.300	[100]	[100]	V <sub>B1</sub>	$\rho V^2 = c_{11}$	8.939	9.002	9.069	9.103	9.128	9.150
		[010]	V <sub>B2</sub>	$\rho V^2 = c_{66}$	4.667	4.709	4.763	4.786	4.814	4.832
		[001]	V <sub>B3</sub>	$\rho V^2 = c_{55}$	4.809	4.842	4.885	4.912	4.934	4.946
		[010]	V <sub>B4</sub>	$\rho V^2 = c_{22}$	7.664	7.704	7.756	7.788	7.810	7.831
		[001]	V <sub>B5</sub>	$\rho V^2 = c_{44}$	4.631	4.673	4.733	4.774	4.799	4.814
3.329	[001]	[100]	V <sub>B6</sub>	$\rho V^2 = c_{66}$	4.645	4.692	4.753	4.788	4.806	4.815
		[001]	V <sub>B7</sub>	$\rho V^2 = c_{33}$	8.062	8.119	8.182	8.222	8.250	8.272
		[100]	V <sub>B8</sub>	$\rho V^2 = c_{55}$	4.921	4.931	4.948	4.962	4.971	4.980
		[010]	V <sub>B9</sub>	$\rho V^2 = c_{44}$	4.634	4.663	4.704	4.727	4.740	4.747
		Quasi-long.	V <sub>B10</sub>	$\rho V^2 = c_{44}$	7.915	7.975	8.042	8.092	8.133	8.166
3.315 3.327 3.308	[011] [101] [110]	Quasi-long.	V <sub>B11</sub>	$\rho V^2 = c_{44}$	8.438	8.511	8.584	8.627	8.665	8.701
		Quasi-long.	V <sub>B12</sub>	$\rho V^2 = c_{44}$	8.450	8.515	8.576	8.613	8.650	8.686

$$c \quad \rho V^2 = \frac{c_{55}}{2} + \frac{c_{33} + c_{11}}{4} + \frac{[(c_{33} - c_{11})^2 + 4(c_{33} + c_{55})^2]^{1/2}}{4}$$

$$d \quad \rho V^2 = \frac{c_{66}}{2} + \frac{c_{11} + c_{22}}{4} + \frac{[(c_{11} - c_{22})^2 + 4(c_{11} + c_{66})^2]^{1/2}}{4}$$

$$a \quad \rho V^2 = \frac{c_{44}}{2} + \frac{c_{23} + c_{11}}{4} + \frac{[(c_{33} - c_{11})^2 + 4(c_{31} + c_{44})^2]^{1/2}}{4}$$

$$b \quad \rho V^2 = \frac{c_{44}}{2} + \frac{c_{23} + c_{33}}{4} + \frac{[(c_{22} - c_{33})^2 + 4(c_{23} + c_{44})^2]^{1/2}}{4}$$

of two dunites with different patterns of olivine orientation. To a first approximation, the elastic properties of the anisotropic dunites are expressed in terms of the elastic constants of hexagonal and orthorhombic materials. The Voigt-Reuss-Hill averaging scheme is used to define the isotropic elastic properties of dunite and the results are compared with simple directional averages that have been applied previously to dunites. The calculated isotropic elastic properties of the dunites are compared with those calculated from olivine single-crystal data.

#### DATA

Two samples of dunite with different fabrics from the Twin Sisters peaks, Washington, were selected for the study. Olivine fabric diagrams are shown in Figure 1 for the two specimens. The olivine orientations were obtained by standard universal stage techniques from several thin sections cut from different parts of each sample. For both rocks the fabrics appear to be relatively homogeneous.

Cores 2.5 cm in diameter and 5 to 7 cm in length were cut from the samples. Directions for each core were assigned using a conventional Miller indices notation for three orthogonal axes ( $x_1$ ,  $x_2$ ,  $x_3$ ) shown in Figure 1. In sample A,  $x_3$  was taken to be parallel to the olivine  $a$  axis concentration and  $x_1$  and  $x_2$  were located arbitrarily in the plane normal to  $x_3$ . For sample B,  $x_1$ ,  $x_2$ , and  $x_3$  were assigned parallel to the maximum concentrations of olivine  $a$ ,  $b$ , and  $c$  axes, respectively.

Average modal analyses from several thin sections are given in Table 1. Chemical analyses of the two samples obtained by standard X-ray fluorescence and atomic absorption techniques are reported in Table 2. The trimmed ends of the cores used for the velocity measurements were crushed for the chemical analyses. Thus the analyses should be fairly representative of the whole rocks.

The technique of velocity measurement is similar to that described by Birch [1960]. Barium titanate transducers of 2-MHz frequencies were used to generate and receive the longitudinal waves. AC-cut quartz transducers of 1-MHz frequencies were used for the transverse wave velocity measurements. At pressures above a few kilobars, accuracies are estimated to be  $\pm 1/2\%$  for  $V_p$  and  $\pm 1\%$  for  $V_s$ . [Christensen and Shaw,

1970]. Pressure was obtained by measuring the change in electrical resistance of a calibrated manganin coil and is accurate to  $\pm 1\%$ .

Compressional and shear wave velocities are given in Table 3. Bulk densities were calculated from the weights and dimensions of the cores. The velocities have been corrected for change in length due to compression by using an iterative routine and dynamically determined compressi-

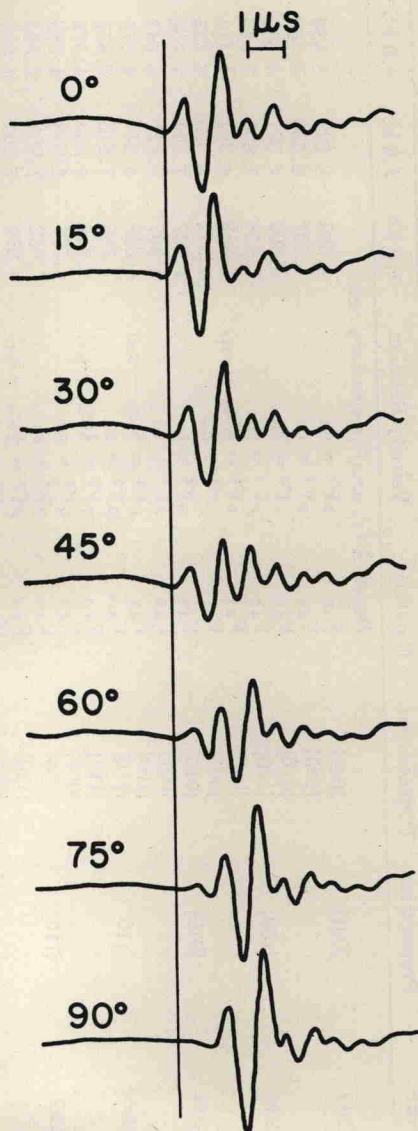


Fig. 2. Oscilloscope traces for shear-wave propagation at 5 kb normal to the olivine  $a$  axes maximum in dunite A.